NASA TECHNICAL MEMORANDUM

NASA TM X- 64630

GYROSCOPE RELATIVITY EXPERIMENT

Rudolf Decher
Space Sciences Laboratory

October 18, 1971

NASA

George C. Marshall Space Flight Center
Marshall Space Flight Center, Alabama

MSFC - Form 3190 (Rev June 1971)

TECHNICAL REPORT STANDARD TITLE PAGE

1. REPORT NO.	2. GOVERNMENT ACCESSION NO.	3. RECIPIENT'S CATALOG NO.
TMX X- 64630		

4. TITLE AND SUBTITLE	5. REPORT DATE
Gyroscope Relativity Experiment	October 18, 1971
	6. PERFORMING ORGANIZATION CODE
7. AUTHOR(S)	8. PERFORMING ORGANIZATION REPORT
Rudolf Decher	
9. PERFORMING ORGANIZATION NAME AND ADDRESS	10. WORK UNIT NO.
George C. Marshall Space Flight Center Marshall Space Flight Center, Alabama 35812	11. CONTRACT OR GRANT NO.
	13. TYPE OF REPORT & PERIOD COVERED
12. SPONSORING AGENCY NAME AND ADDRESS National Aeronautics and Space Administration Washington, D. C. 20546	Technical Memorandum
	14. SPONSORING AGENCY CODE

15. SUPPLEMENTARY NOTES

Prepared by Space Sciences Laboratory, Science and Engineering

16. ABSTRACT

A gyroscope test of general relativity theory has been proposed by a group of investigators at Stanford University. This report discusses the basic ideas and hardware concepts conceived by the investigators to implement the experiment. The goal is to measure the extremely small relativistic precession of gyroscopes in an earth-orbiting satellite. The experiment hardware (cryogenic gyroscopes, a telescope and superconducting circuits) is enclosed in a liquid helium dewar. The experiment will operate in orbit for about one year.

17. KEY WORDS	18. DISTRIBUTION STATEMENT
	Unclassified, Unlimited Eugene W. Urban for Rudolf Decher, Space Sciences Laboratory

19. SECURITY CLASSIF. (of this report)	20. SECURITY CLASSIF. (of this page)	21. NO. OF PAGES	22. PRICE
Unclassified	Unclassified	40	$3.00

MSFC - Form 3292 (May 1969)

TABLE OF CONTENTS

LIST OF ILLUSTRATIONS

TECHNICAL MEMORANDUM

GYROSCOPE RELATIVITY EXPERIMENT

INTRODUCTION

This report describes concepts and ideas for implementation of the Gyroscope Relativity Experiment. During the development of the experiment and laboratory hardware, certain changes in the concept of implementation can be expected. Therefore, the description given in this report should be considered a typical approach. Alternate solutions are under investigation in several areas.

The goal of the gyro relativity experiment is a test of general relativity theory to be accomplished by measuring the relativistic precession of gyroscopes in an earth-orbiting satellite. The experiment has been under development for several years by a group of scientists associated with the Physics and the Aeronautics and Astronautics Department of Stanford University. Prime investigators at the present time include W. M. Fairbank, C.W.F. Everitt, and D. B. DeBra. The gyroscope test of general relativity theory was conceived by L.I. Schiff in 1960; the implementation using cryogenic techniques and a satellite mission was suggested by R. H. Cannon, W. M. Fairbank, and L. I. Schiff. A preliminary proposal to NASA for a satellite experiment was first made in January 1961 by Fairbank and Schiff and was followed by an official proposal in November 1962.

Work on the gyro relativity experiment has been supported jointly by NASA and the Air Force under a program to develop a drag-free satellite and the cryogenic technology for the relativity experiment. The drag-free satellite, which became a separate project in 1968, includes a test flight of the zero-g control principle on a Navy satellite. The development of the relativity experiment has been sponsored by NASA/OSSA since 1963 under a NASA grant to Stanford University. Marshall Space Flight Center, involved in the project since 1965, has provided assistance to the experiment investigators and aided in the planning of space flight testing of experiment systems. More recently, the Center provided support in precision mechanical manufacturing and testing, and the development of the superconducting gyroscope.

The technology under development for this experiment represents advancement of the state of the art in several areas; e.g., in gyro technology,

pointing accuracy of star tracking telescopes, cryogenic environment in space (liquid helium dewar), sensitive magnetometer (gyro readout circuit), and precision manufacturing and measuring techniques. This advanced technology will have applications in future space missions, particularly for space astronomy.

EXPERIMENT DESCRIPTION

Relativistic Gyro Precession

In 1960, L. I. Schiff [1] proposed a new experimental test of Einstein's general relativity theory which would permit a decision between Einstein's theory and other more recent theories of gravitation. According to Schiff's calculations, based on Einstein's theory, a gyroscope with a torque-free and exactly spherical rotor located in an earth satellite will experience a small precession of its spin axis in an inertial coordinate frame referenced to the stars. In the Newtonian theory of gravitation, the spin axis of such a torque-free, spherical gyro would remain fixed in space. The relativistic precession of a gyro in an earth satellite is given by the following equations [1]:

$$\frac{d\bar{S}}{dt} = \bar{\Omega} \times \bar{S} \quad , \tag{1}$$

$$\bar{\Omega} = \frac{3GM}{2c^2 r^3} (\bar{r} \times \bar{v}) + \frac{GI}{c^2 r^3} \left[\frac{3\bar{r}(\bar{\omega}\,\bar{r})}{r^2} - \bar{\omega} \right] \quad , \tag{2}$$

where

S = angular momentum of the gyro,
Ω = angular velocity of the precession,
M = mass of the earth,
I = moment of inertia of the earth,
G = gravitational constant,
c = velocity of light,
ω = angular velocity of earth rotation,
r = radius from earth center to the satellite.

From equation (1) it follows that the angular momentum S of the gyro precesses with the angular velocity Ω while the magnitude of S stays constant. The relativistic precession is composed of two components represented by the two terms of equation (2).

The first term of equation (2) is the geodetic precession caused by the orbital motion of the gyro. The geodetic precession depends on the velocity v with which the gyro moves through the gravitational field of the earth. A gyro located on the earth's surface moves with the rotation of the earth, and the geodetic precession would amount to 0.4 arc sec per year (at the equator). For a gyro orbiting in an 800-km (500-n.mi.) circular orbit, the precession is increased to about 7 arc sec per year. The spin axis of the gyro turns slowly in the same direction as the gyro moves in orbit. For a circular orbit with radius r, the vector product $\overline{r} \times \overline{v}$ of equation (2) yields $2\pi r^2$ for one orbital revolution. Thus, the geodetic precession amounts to 3π GM/c^2r radians per revolution in orbit decreasing with 1/r as the height of the orbit increases. Since a gyro in a low-earth orbit moves around the earth several times per day, its geodetic precession over a period of time is increased compared to an earth-bound gyro. The geodetic precession may be viewed as a weak tendency of the gyro to align its spin axis with the gravitational field lines. The net effect for an orbiting gyro is the slow rotation of the spin axis.

The second term in equation (2) is called the motional precession. It is caused by the rotation of the earth on its axis and is independent of the motion v of the gyroscope. This effect may be illustrated in the following way: the rotating earth drags its gravitational field around. A gyro with its spin axis at right angle to the earth axis has some tendency to align its spin axis with the gravitational field rotating with the earth. The integrated effect for an orbiting gyro is a slow precession of the spin axis in the direction of earth rotation. The motional precession is smaller than the geodetic precession; but, from a scientific viewpoint, it is the more interesting one since it represents the only known influence of mass rotation on gravitation. The motional precession for a gyroscope in a circular polar orbit of 800 km (500 n.mi.) is approximately 0.05 arc sec per year.

Figure 1 shows the situation for 2 gyroscopes (spherical rotors) in a circular polar orbit of 800 km (500 n.mi.). At the beginning of the experiment (t = 0) the spin axis of Gyro 1 is parallel to the earth axis. After 1 year, the spin axis of this gyro has rotated in the plane of the orbit and in the direction of orbital motion by about 7 arc sec as a result of the geodetic precession.

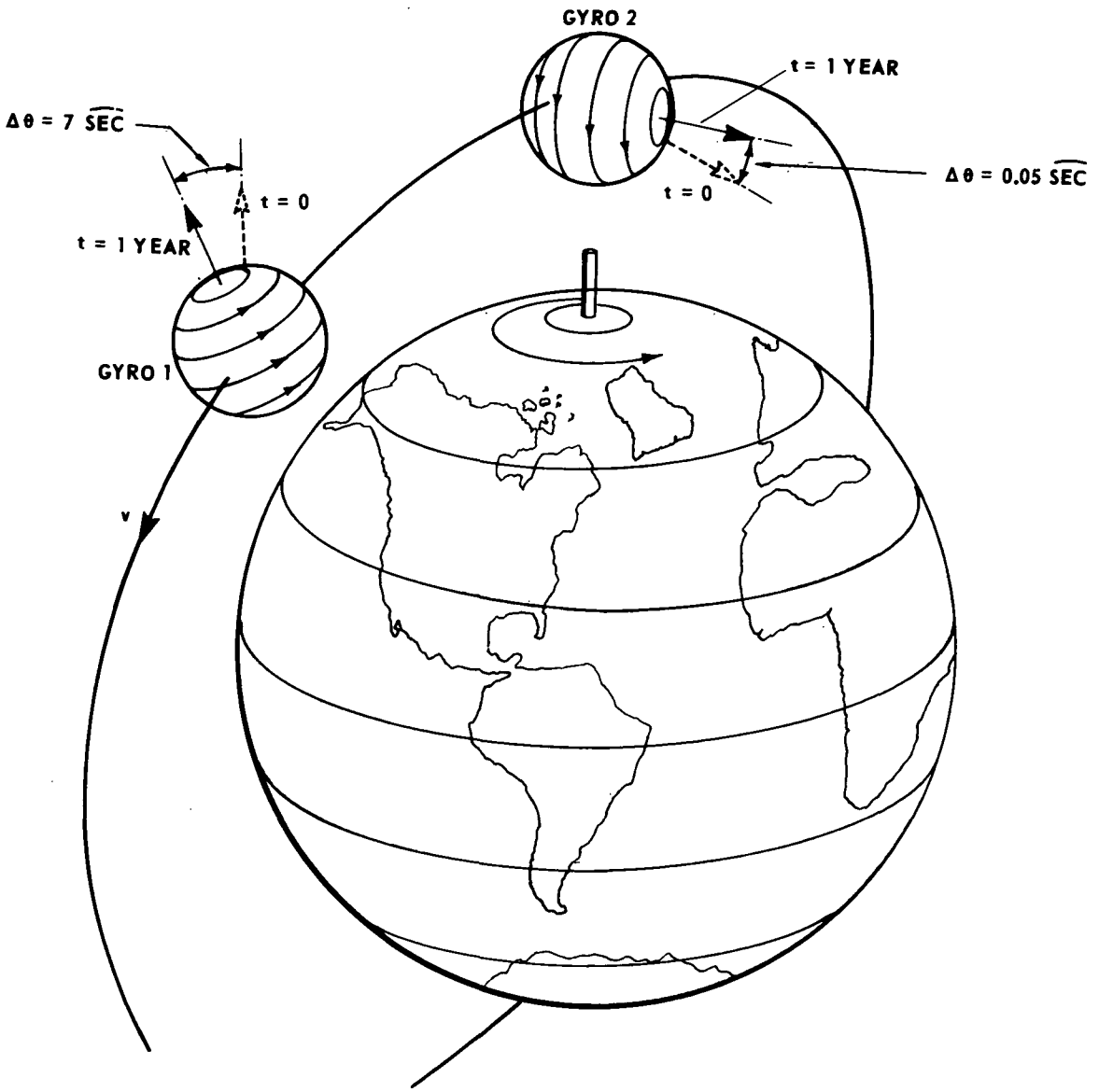

Figure 1. Relativistic gyro precession.

The spin axis of Gyro 2 is initially oriented at right angle to the orbit plane and the earth axis. The motional effect causes a precession of Gyro 2 of 0.05 arc sec per year about an axis parallel to the earth axis. In circular polar orbit and with spin axis orientations as shown in Figure 1, the two relativistic precession effects can be measured separately since the spin axis of Gyro 1 is not influenced by the earth rotation and the spin axis

of Gyro 2 is not affected by the orbital motion. The relativistic effect of the masses of the sun and the moon on the gyro spin axis, compared with the effect from the earth, can be neglected.

Experiment Concept

Because of the extremely small relativistic gyro precession, this experiment can be performed only in space. The motional precession is about the same magnitude for a gyro on earth as for a gyro in orbit. However, the geodetic precession for an orbiting gyro is much larger than for a gyro on the earth's surface. On the ground, gravity and other disturbing forces as well as the strong support forces required to suspend the gyro in the g environment will cause drift rates that are several orders of magnitude larger than the effects to be measured. The analysis has shown that in the zero-g environment in space and with the use of cryogenic technology the disturbances on the gyro and related experiment systems can be made small enough to permit the measurement of the relativistic gyro precession.

The proposed gyro relativity experiment will use extremely precise, unconventional gyroscopes in a satellite in a circular polar orbit of about 800 km (500 n.mi.). For this orbit the relativistic spin axis motion amounts to:

6.9 arc sec per year for the geodetic precession
0.05 arc sec per year for the motional precession.

To measure the relativistic gyro drift, the spin axis orientation of each of several gyroscopes in the satellite is compared over a period of time with the line-of-sight to a reference star provided by a star-tracking telescope. The measurement of such a small gyro precession cannot be accomplished with conventional gyro technology. Improvements of many orders of magnitude would be required. To measure the motional precession to an accuracy of 2 percent requires a drift rate of 0.001 arc sec/year (1.6×10^{-16} radians/sec) or less for the gyro. The drift rate of 0.001 arc sec/year has been adopted as the desirable goal for the gyro design. A thorough theoretical analysis has shown that such a low drift rate is possible in principle with the gyro concept selected for this experiment and in the zero-g and cryogenic environment. Some advancements in the state of the art in certain areas are necessary to accomplish this goal. Several of these

advancements have been achieved, while others are in progress. However, a worthwhile relativity experiment could still be performed with a gyro drift rate of 0.1 arc sec/year; this would permit the measurement of the geodetic precession with an accuracy of about 1.5 percent.

Fundamental design requirements for this experiment and in particular for the gyro are:

1. Reduction (elimination) of all nonrelativistic torques to achieve the design goal of 0.001 arc sec/year.

2. Development of a spin-axis readout method with sufficient null stability and sensitivity to measure the small relativistic precession without a reacting torque on the gyro.

Based on calculations, it is believed that the gyro concept described below will meet these requirements. Testing of the first gyro model will start in the near future.

The gyro rotor is a solid quartz ball 38 mm (1.5 in.) in diameter with utmost sphericity and uniformity in density. The rotor, which is coated with a thin layer of superconducting niobium, is suspended inside the gyro housing in an electrical field generated by three pairs of electrodes. The rotor spins at about 200 revolutions per second (12,000 rpm) in vacuum. Spin-up of the rotor is accomplished by a helium gas jet. Readout of the spin-axis orientation utilizes the magnetic moment generated by a rotating superconductor (London moment). This magnetic moment is parallel to the instantaneous spin axis. The gyro precession is determined by measuring the change of magnetic flux from the London moment through superconducting loops in the gyro housing with a unique, highly stable and sensitive magnetometer. The quartz gyro housing is enclosed in a superconducting magnetic shield to eliminate external magnetic fields.

To achieve the accuracies as discussed above, the relative alignment of gyro and telescope components must be maintained to the highest degree possible. Changes could be caused by thermal expansion and material creep. Creep of materials is drastically reduced under zero-g in space and at cryogenic temperature. The thermal expansion problem can be overcome by proper selection of materials and the cryogenic environment applied to the whole experiment. The implementation of this experiment to the required accuracy without cryogenic technology would be hopeless. The whole experiment (gyros, telescope, and connected critical components) is enclosed in

a liquid helium dewar operating at 1.6° K during the lifetime of the experiment. The cryogenic cooling provides the low temperature required for operation of the superconducting gyros and magnetic shield as well as temperature stabilization for the experiment systems. Telescope and gyroscope parts are made of quartz which has a very low thermal expansion coefficient at this low temperature. All of these quartz parts are joined together by optically contacted surfaces to avoid interface problems with different materials. Quartz is an ideal material for the gyro rotor because it can be made with high homogeneity and purity. All experiment components must be made of very highly-nonmagnetic materials.

Relativity Satellite

The experiment hardware for the relativity experiment consists of four gyroscopes, a proof mass sensor, a star-tracking telescope, associated electronics, and a liquid-helium dewar enclosing the experiment system. The concept of a relativity satellite is depicted in Figure 2.

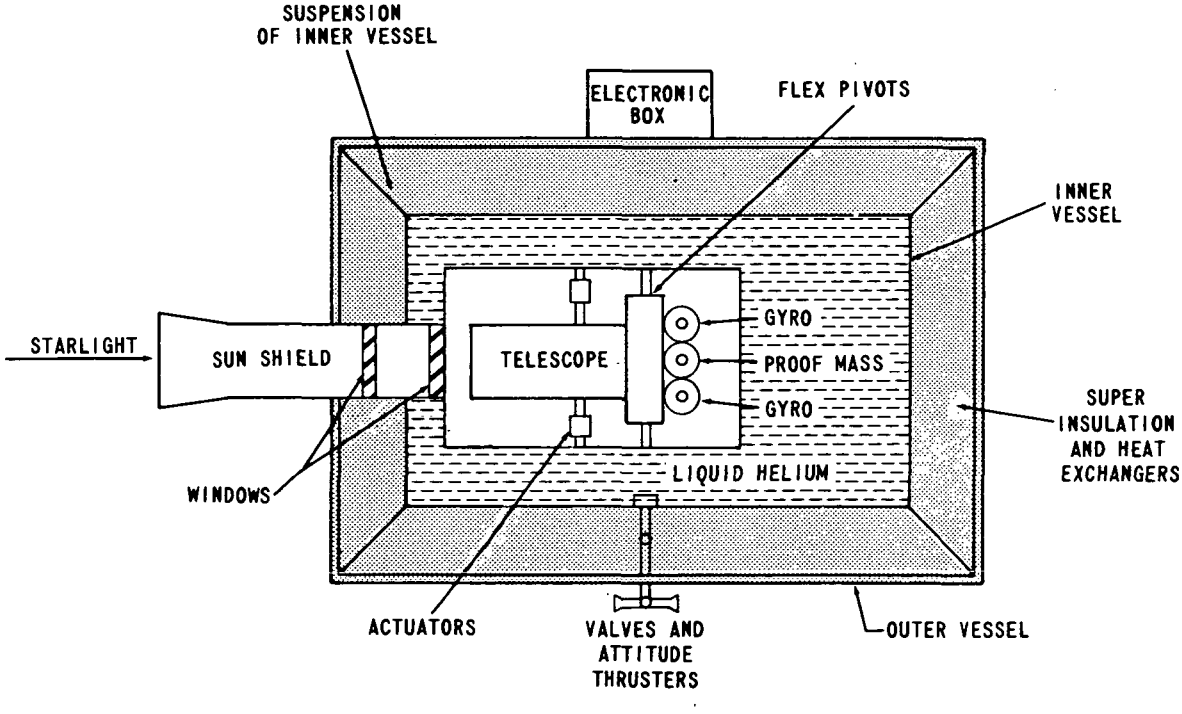

Figure 2. Relativity satellite concept.

The light from the reference star enters the telescope through heat-reflecting windows. The star-tracking telescope provides the reference direction for measurement of the gyro precession. Four gyros, providing redundant readout, are mounted to the rear of the telescope. The proof mass sensor located at the center of mass of the satellite generates the signals for translation control of the satellite to achieve zero-g environment in the satellite (compensation of air drag). The liquid-helium dewar maintains a temperature of 1.6° K in the experiment space. The inner vessel of the dewar is suspended in the outer vessel by thin wires or tapes to reduce heat transfer. The space between the two vessels is filled with superinsulation and contains heat exchangers for the helium gas boiling off from the inner vessel. The inner vessel contains the liquid helium and the experiment systems. The experiment block (telescope plus gyros) is mounted inside the helium vessel on flex pivots which in connection with cryogenic actuators permit fine attitude control and pointing. The boil-off helium gas is used for attitude control of the satellite. Twelve jet nozzels provide continuous venting, attitude control, and translational control (zero-g control). The supply of liquid helium (about 140 Kg) will be sufficient to keep the experiment in operation for at least 1 year. The major portion of the experiment electronics is contained in a box outside the dewar. The superconducting circuits and associated low-noise amplifiers are located inside the cryogenic experiment space.

The arrangement of the four gyroscopes around the proof mass as indicated in Figure 2 is one of several possible configurations. In another arrangement, all gyros could be located along the roll axis (telescope axis). There are several possibilities for orientation of the gyro spin axes. For example, two gyro spin axis could be aligned parallel to the earth axes; the remaining two gyros would have their spin axis at right angles to the orbital plane (as shown in Fig. 1). With this configuration, the geodetic and the motional precession could be measured separately. To average out some of the unwanted residual torques on the gyros and for other reasons, a continuous very slow roll motion of the satellite about the telescope axis (one revolution in several hours) would be a big advantage. In connection with this mode of operation, different orientations of gyro axes are under consideration. For example, two gyro axes parallel to the telescope axis, one gyro axis parallel to the earth axis, and one axis perpendicular to the orbit plane. In this configuration each of the two relativistic precession effects is measured by three gyroscopes.

An artist's concept of the relativity satellite is shown in Figure 3 (from a mission study by Ball Brothers Research Corp.). The cylindrical

portion of the satellite is the helium dewar. The spacecraft systems (i.e., solar panels, batteries, and electronic systems) are mounted on a ring around the dewar. This design would permit independent handling of spacecraft and experiment systems.

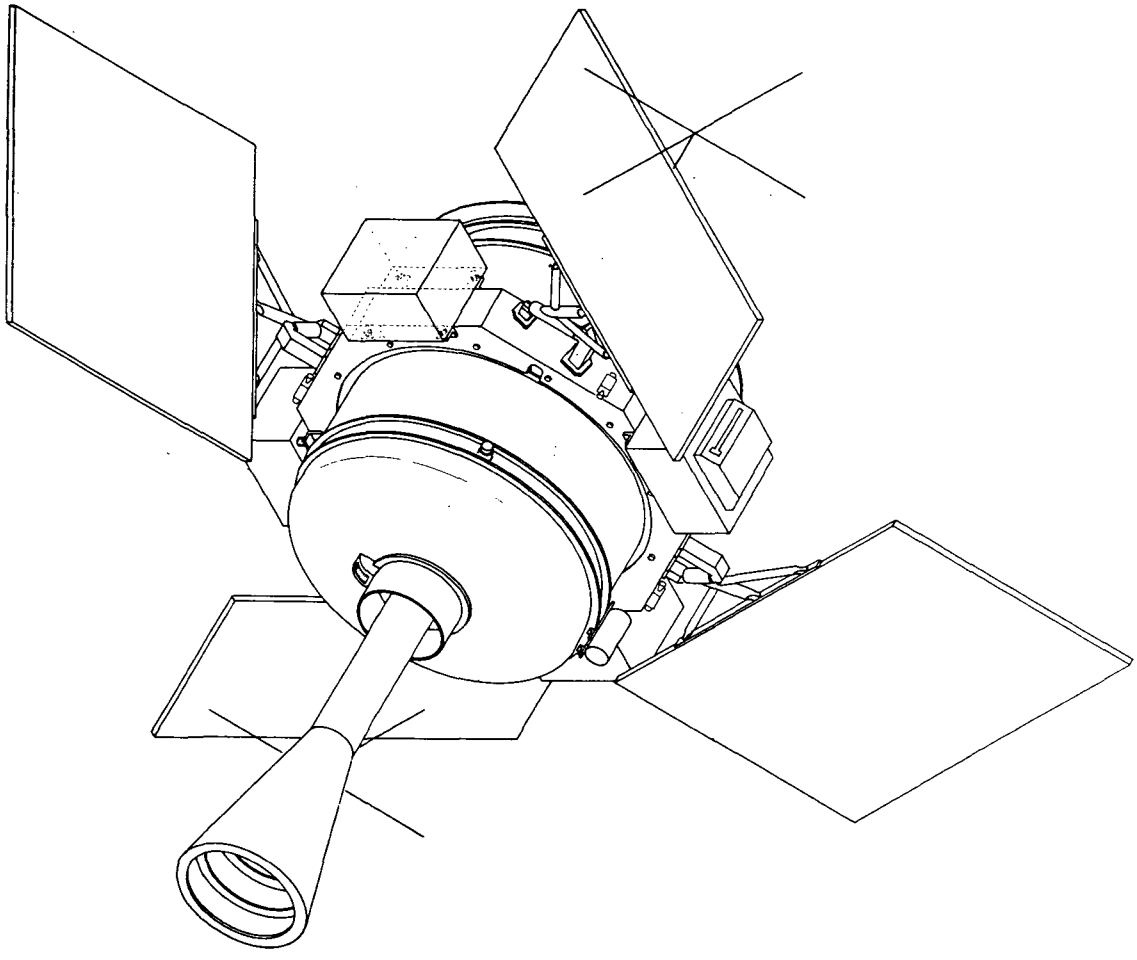

Figure 3. Satellite configuration.

Experiment Development

Manufacturing of the telescope has been completed. Extensive testing of the detection system has been performed, and a resolution of 0.01 arc sec has been achieved with one second integration time. Greater

resolution will be obtained by integration over longer time periods.

Testing of two gyro models will begin soon. Following these early tests a laboratory simulation of the experiment will be built up in steps. The laboratory dewar with the telescope and one or two gyros will be supported in a telescope mount to track Polaris or an artificial star. In a later phase, simulation of attitude control will be added. The free-flight performance of the gyro cannot be tested directly on the ground. Testing in the 1-g gravity environment will be affected by large torques on the gyroscope. A test flight of two gyros in orbit together with data from ground testing will permit to assess the real performance of the gyro. An orbital test flight of a small liquid helium dewar (equipped with the fundamental features of the final dewar) will be required before a gyro test flight.

An error analysis has been going on simultaneously with the development of the experiment at Stanford University. A summary of the results obtained so far has been published by C. W. F. Everitt [2].

GYROSCOPE

Mechanical Design

The relativity gyro design is derived from the electrically supported gyro (ESG) developed by Honeywell, Inc. The basic ideas of an ESG were developed by A. Nordsieck and his colleagues at the University of Illinois in 1953.[1]

The cryogenic relativity gyro operates at the temperature of liquid helium (1.6°K). The rotor is a solid quartz ball, 38 mm (1.5 in.) in diameter, coated with a thin layer 10 μ (1000 Å) of superconducting niobium. A superconducting rotor is required for the spin axis readout method utilizing the London moment. The rotor is supported in the evacuated gyro housing in an electrical field generated by 3 pairs of electrodes. The drift performance of the gyro depends primarily on the perfectness of the rotor ball with respect to homogeneity and sphericity. To achieve the desired low drift rates of the gyro (0.001 arc sec/yr) the quartz ball should meet the following requirements:

1. The spin-up and readout of the relativity gyro are totally new concepts developed by the group at Stanford University.

Sphericity	$\Delta r/r = 1 \times 10^{-6}$ or less
Homogeneity in density	$\Delta\rho/\rho = 1 \times 10^{-6}$ or less

Lapping and polishing technology has been improved (at MSFC) to permit the manufacturing of quartz balls with a sphericity of at least 50×10^{-6} mm (2×10^{-6} in.) which is the limitation of the best existing roundness measuring equipment. Improved measuring techniques are under development. To test the homogeneity of the quartz material to be used for rotor manufacturing, a quartz cube with polished surfaces is made first. The homogeneity of this material is then checked on the basis of optical interference fringes.

Quartz was selected as the material for the rotor and gyro housing because of the low thermal expansion coefficient (particularly at the low temperature) and because it is obtainable with highly uniform density. Other materials, e.g., pure crystalline silicon or cervit, may be considered. Experimental investigations will be necessary to determine if materials other than quartz can meet all requirements (e.g., thermal expansion, homogeneity, magnetic characteristic, matching behavior, etc.).

Two different mechanical designs of the gyro housing have been developed and will be tested in the near future. The first model (designed by Stanford University and Honeywell, Inc.) is shown in Figure 4. The quartz gyro housing consists of two half shells forming the spherical cavity which encloses the rotor ball. The two halves are held together by a quartz ring. The inside view of the gyro housing is given in Figure 5 showing three (circular) electrodes plated on the inside of the cavity, the spin-up gas channel and openings for gas inlet and pumping. The alignment of the two half shells is accomplished by two pins. The gap between the rotor and the housing (i.e., the electrode surfaces) is 38×10^{-3} mm (1.5×10^{-3} in.). The spherical cavity must be manufactured with utmost precision. The gyroscope housing is enclosed in a quartz sphere which is coated on the outside with a superconductor (lead or niobium) to provide a magnetic shield. The gas spin-up and pumping pipes and the electrical connections for the six electrodes penetrate the quartz sphere. A different gyro design (MSFC) is shown in Figure 6. The housing consists of two identical cavities which are less than half spheres to provide space for the spin-up channel. The spin-up channel is formed by two discs between the gyro shells. The four housing parts are centered by a quartz ring which provides support for the spin-up pipes and contains openings corresponding to the exhaust slots in the spin-up discs. The assembly is held together by two rings with screws. All gyro parts are made of quartz.

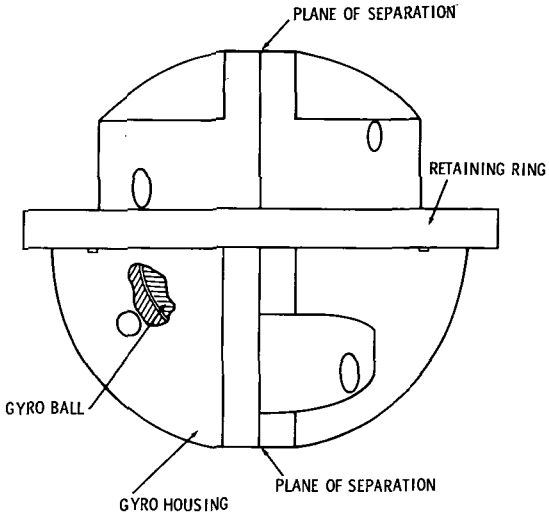

Figure 4. Stanford/Honeywell gyro configuration, outside view.

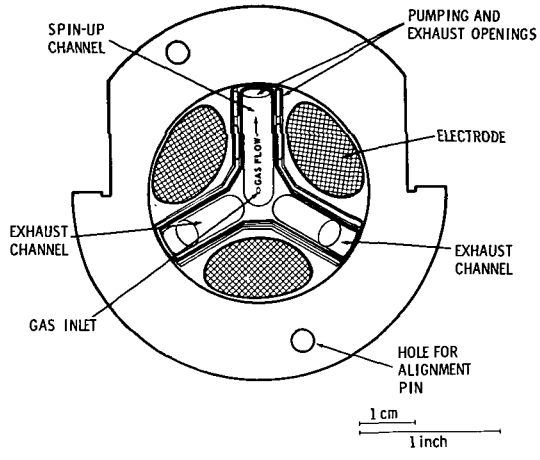

Figure 5. Stanford/Honeywell gyro configuration, inside view.

Electrical Suspension

The gyro rotor is suspended inside the gyro housing by an electrical field generated by six electrodes. The alternate solution to support the superconducting ball in a magnetic field is not feasible with this gyro since any magnetic field would interfere with the magnetic readout of the London moment. The principle of the electrical suspension system was developed by Honeywell, Inc. for the ESG.

The electrodes are circular in shape consisting of titanium deposited onto the inner wall of the gyro housing (Fig. 5). The three pairs of electrodes represent a three-axis system with axes perpendicular to each other. The suspension system performs two functions: it senses the position of the ball and it provides an electric force field to keep the ball centered between the electrodes. The electric suspension system has three independent channels, one for each axis (pair of electrodes). A simplified block diagram is shown in Figure 7. Position sensing of the ball is accomplished by measuring the capacitance between the electrodes and the rotor. The capacitance-sensing bridge operates at a different frequency in each channel (1.2, 1.5, and 1.8 MHz) which is provided by the sensing oscillator. Displacement of

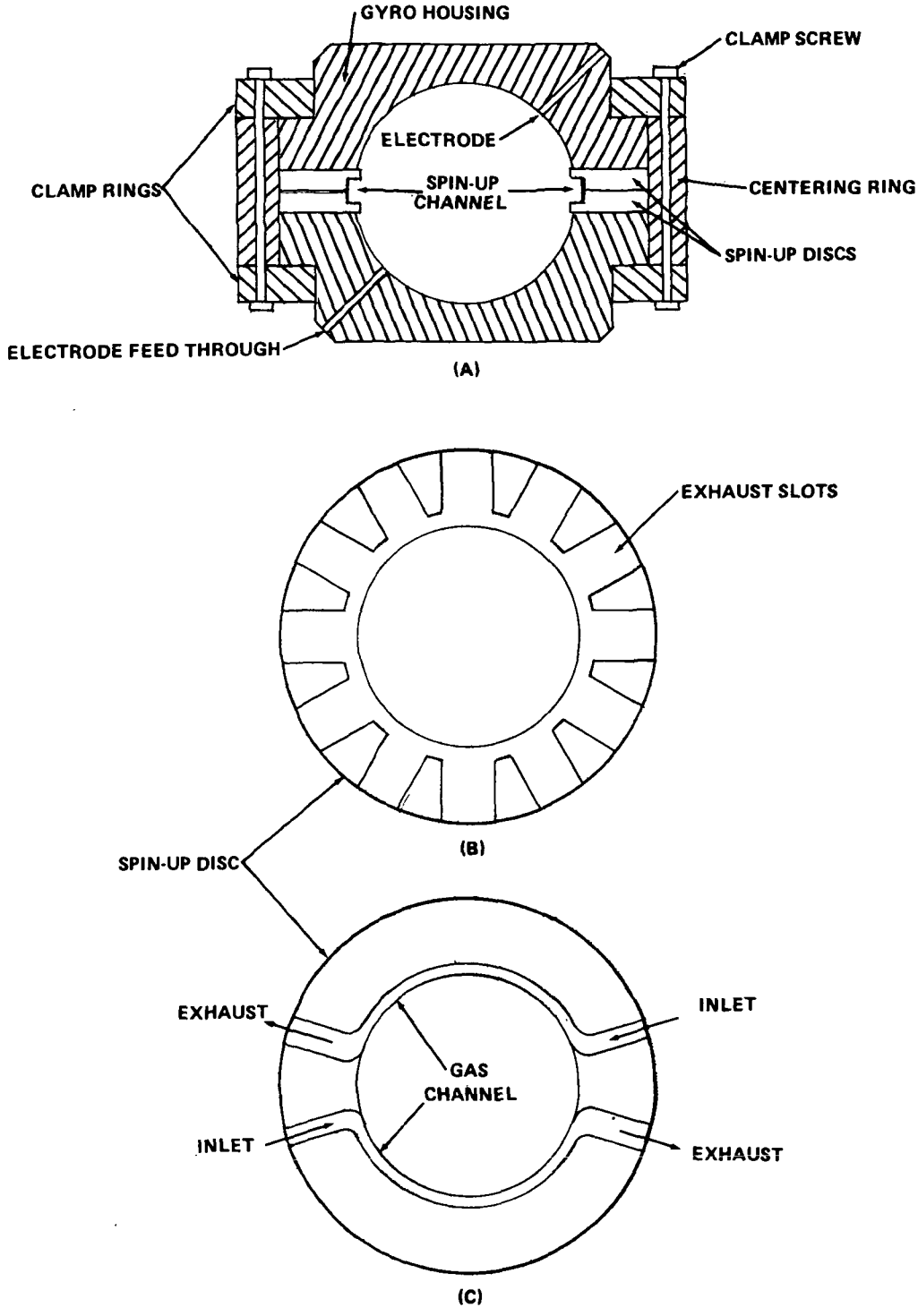

Figure 6. MSFC gyro configuration.

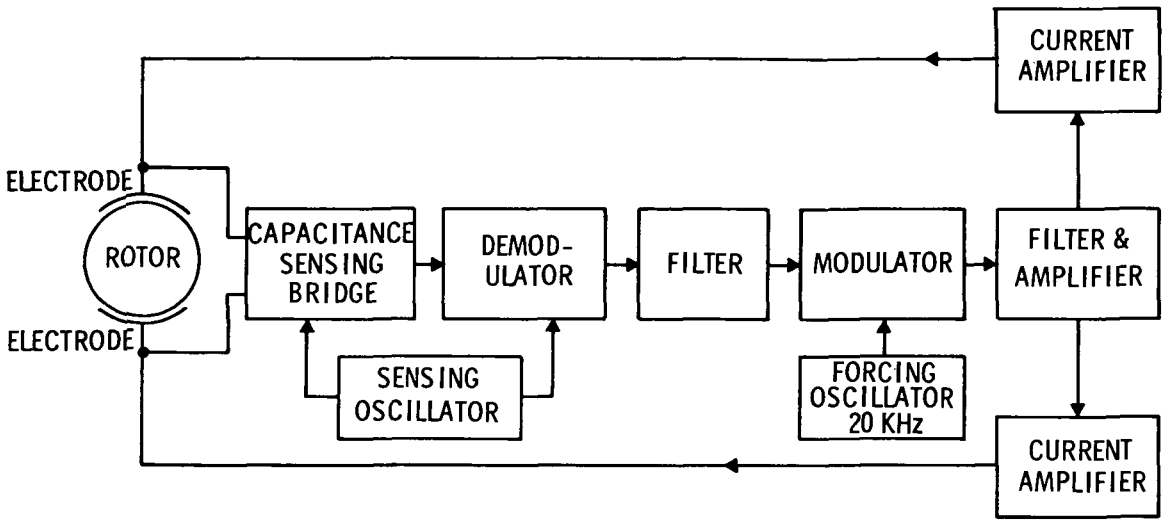

Figure 7. Suspension electronics.

the rotor from the center between electrodes results in a variation of amplitude and phase of the bridge output signal which is demodulated and filtered to generate a control signal for the forcing field. This signal modulates the force field to keep the ball in center position.

The forcing signal is derived from a 20-kHz oscillator which also provides a preload voltage (to obtain linear control) of about 500-V rms between electrode and rotor. The position control signal from the sensing bridge is modulated on the 20-kHz forcing signal, which, after proper filtering, drives two current amplifiers, to generate the supporting force field through output transformers on the electrodes. The sum of the output currents of the two current amplifiers is constant in phase and amplitude (sinusoidal signal). Each output transformer together with the electrode-rotor capacitance and feed-cable capacitance is tuned to resonance (20kHz).

The output transformers feeding the three pairs of electrodes are connected in a three-phase, Y-configuration. The phase relationship is such that the rotor is at the ground potential of the 20-kHz circuits. On the ground, a high voltage at the electrodes is required to support the rotor against gravity. A maximum voltage of about 1500 V rms may appear between electrode and ball across the gap of about 0.04 mm (for 2.5-g support). Voltage breakdown caused by field emission sets an upper limit for the strength of the supporting field at about 5 g for such a system. The electrical

suspension system to be used for ground testing will provide support against 2.5 g. During spin-up on the ground, the gas pressure in the electrode gap must be kept low to prevent electrical breakdown. In orbit, a supporting field of less than one volt will be sufficient. Spin-up of the gyro will be done in orbit because of the limitation of the electrical suspension at high acceleration.

Gyro Spin-Up

Spin-up of the gyro is accomplished by a gas jet. The only alternate solution would be a mechanical clutch which would require a very complex mechanical design and involve the danger of damaging the surface of the rotor. The induction motor principle cannot be used because the rotor must be in a superconducting state before it is spun up to develop the London moment.

The gas spin-up method has been tested on a model [3]. The principle of this method is shown in Figure 8. Each half of the gyro housing contains a channel on the inside surface through which gas flows around the equator of the rotor ball. The friction between the turbulent gas flow in the channel and the surface of the ball applies the torque to the ball. According to the model tests, a spin speed of 200 rps can be achieved in about 30 minutes [3]. The spin-up procedure includes the following steps: first, the gyro is evacuated; second, then the supporting field is switched on to float the rotor; and third, the gas flow is applied to the spin-up channel and the rotor begins to spin.

A spin speed of about 200 rps will be used in the experiment. With higher speeds, the distortion of the ball caused by centrifugal forces increases to undesirable values. The maximum rotor speed obtainable is limited by drag from gas which escapes from the spin-up channel into the gyro housing. Since the magnitude of the magnetic London moment is proportional to the rotational speed of the rotor, a high spin speed is desirable for readout of the spin-axis orientation. A reasonable trade-off between readout sensitivity and ball distortion exists around 200 rps.

The gas for spin-up is generated by boiling off liquid helium from a special chamber in the dewar with an electrical heater. The gas, which has a temperature of about 4°K, passes through a shutoff valve and pipes to the inlet of the spin-up channels. The exhaust of the channels is connected through pipes to the vacuum in space. On the ground a high-speed mechanical pump is connected to the spin-up exhaust. When the desired spin rate has been

achieved, the helium gas flow is cut off by the valve, and the rotor continues to spin in vacuum. During space flight, a vacuum of at least 10^{-9} mm Hg is maintained. The gas drag at this low pressure will be so small that the spin rate will decrease only by a small amount during operation of the experiment (1 year). The spin rate is monitored by the measurement of the magnetic flux (generated by the London moment) through the readout loops.

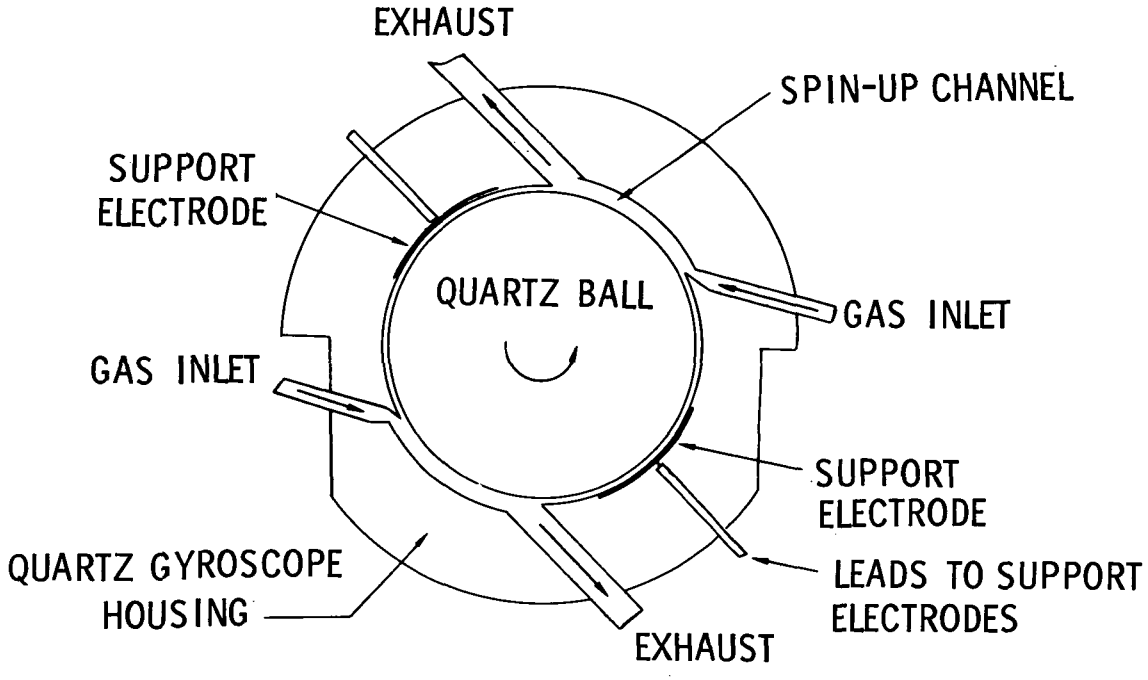

Figure 8. Gyro gas channels.

A pressure of about 16 mm Hg is required in the channel to achieve the necessary gas-flow velocity for spin-up. The gas pressure in the electrode area must stay below 0.025 mm Hg (at 4.2°K and for a 1 g support field) to avoid electrical breakdown. To restrict the gas flow to the spin-up channel; i. e., to reduce the escape of gas into the electrode area, the edges along the spin-up channel are raised above the inside surface of the gyro housing, thereby generating a narrow gap of about 5×10^{-3} mm (0.2×10^{-3} in.) between the ball and spin-up channel edge. In addition, auxiliary pumping slots are provided on each side of the spin-up channels.

Figure 9 shows a cross section through the gyro housing and spin-up channel for the Stanford/Honeywell gyro model. As can be seen in Figure 5, the electrodes are surrounded by the raised channel edge to restrict the gas flow. The spin-up channel in each gyro half shell extends over an arc of approximately 90 degrees. The three-arm channel arrangement (Fig. 5) gives dielectric symmetry for a uniform suspension field.

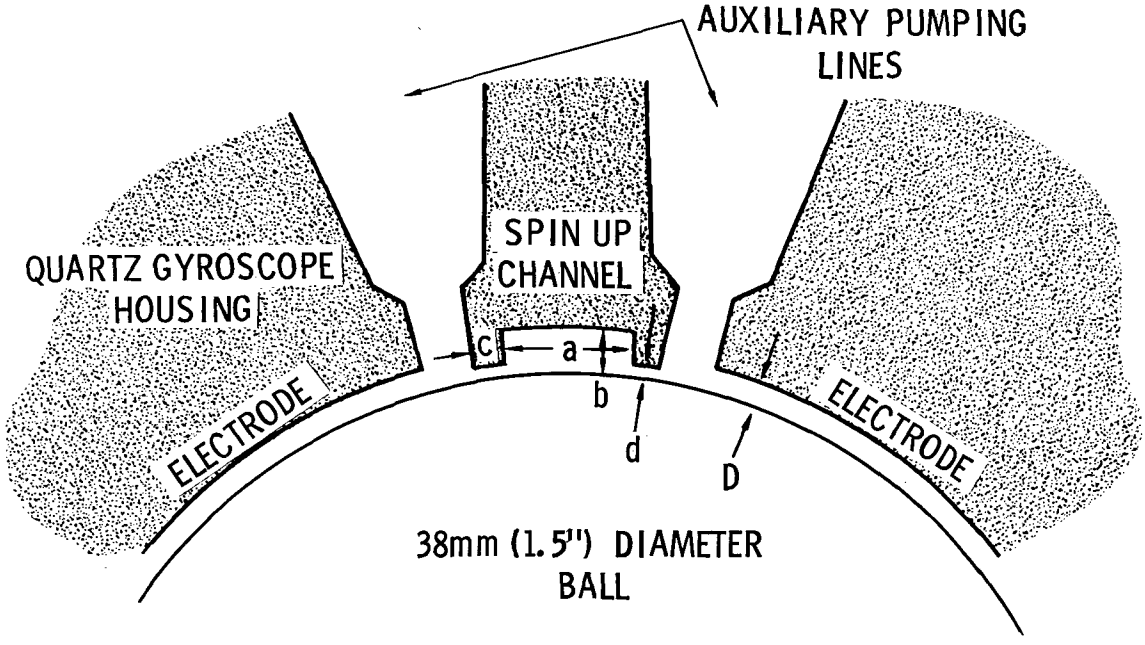

a: 5mm(0.2")
b:0.5mm(0.02")
c:0.5mm(0.02")

d: 5×10^{-3} mm (0.2×10^{-3} inch)
D: 38×10^{-3} mm (1.5×10^{-3} inch)

Figure 9. Stanford/Honeywell model spin-up channel cross section.

A cross section through the MSFC gyro model is shown in Figure 10. The spin-up channel is made up by the two spin-up discs sandwiched between the halves of the gyro housing. Either the two-channel arrangement shown in Figure 6(C) or one spin-up channel all the way around may be used. Auxiliary exhaust slots are provided in each spin-up disc at the interface with the gyro housing [Fig. 6(B)].

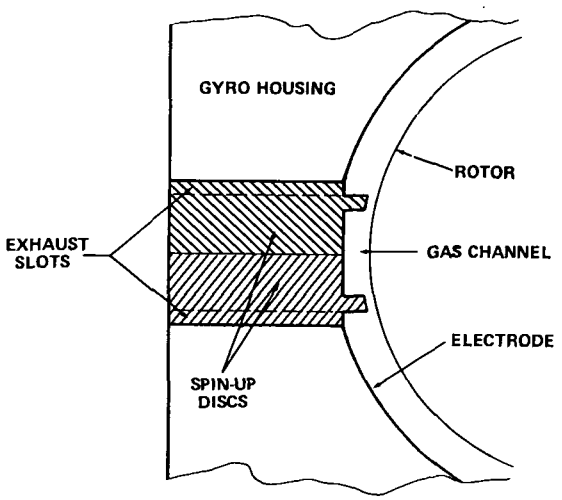

Figure 10. MSFC model spin-up channel cross section.

The problem of electrical breakdown does not exist in space because the suspension voltage can be reduced to a very low value. The high-suspension voltage is required on the ground to support the ball against earth gravity. Mainly because of the g limitation of the electrical suspension gyro, spin-up will be initiated after the experiment is in orbit.

Spin Axis Readout

The problem of torque-free spin axis readout has been solved by cryogenic technology. A rotating superconductor generates a magnetic moment parallel to its spin axis. When the superconducting gyro rotor is spun up, the electrons in the niobium coating of the ball will lag (because of their inertia) behind the accelerated atomic latice of niobium since they can move without resistance in the superconductor. The net effect is a ring current around the surface of the ball which results in a magnetic moment (London moment). The magnetic moment of the rotor is always parallel to the instantaneous spin axis (Fig. 11). By measuring the magnetic flux through a loop around the ball, the precession of the spin axis, with respect to the plane of the loop (assuming constant spin rate), can be determined. The magnetic field H of the London moment is given by:

$$H = 10^{-11}\,\omega\ [\text{tesla}] = 10^{-7}\omega\ [\text{gauss}] \quad ,$$

where ω is the spin rate in rad/sec. For the gyro rotor, spinning at 200 rps, the magnetic flux through the area of the ball ($\sim$ readout loop)

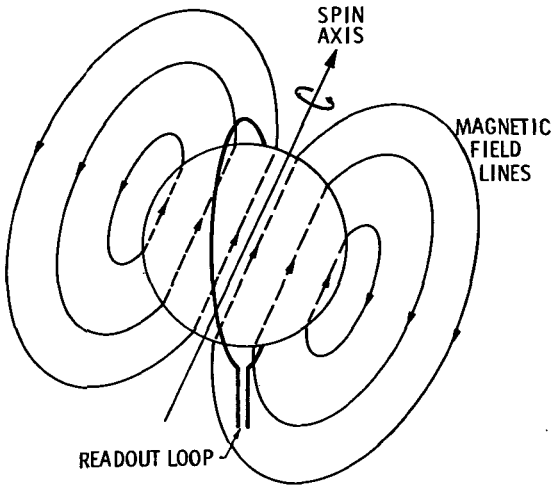

Figure 11. London moment.

is 1.4×10^{-3} weber (gauss cm^2). The gyro housing contains two or three readout loops, each connected to a very sensitive magnetometer to measure the motion of the gyro spin axis and to monitor the spin speed.

If a readout accuracy of 0.001 arc sec is desired, the magnetometer must be capable of detecting flux changes of the magnitude of 10^{-12} weber (gauss cm^2). A Josephson junction-type magnetometer is capable of performing the measurement with proper integration time.

To achieve utmost stability and sensitivity in the gyro readout, a unique magnetometer is under development at Stanford University [4]. The principle of operation may be explained with the aid of Figure 12. The magnetometer consists of two superconducting loops connected in series (the gyro readout loop around the ball and the modulator loop outside the gyro housing). The magnetic flux through a closed-loop superconductor stays constant; i.e., a current once introduced in the loop continues to flow unchanged. If an external field is applied or changed, the current in the loop will change in such a way to counterbalance the change from the external field to keep the magnetic flux through the loop constant. The continuous small relativistic precession of the rotor spin axis causes a change of the DC current in the loop which is transformed into an AC current and read out by a nulling method.

The AC signal is generated by modulating the inductance of the modulator loop. The inductance modulator consists of a meandering superconducting niobium lead plated on the surface of a glass flat. The width of the conductor is 10 μ with a total length of 5 m folded into an area of about 1×1 cm. A small distance above this circuit, a superconducting ground plane vibrates at a frequency of 100 kHz, driven by an oscillating quartz crystal (Fig. 12). The result is a modulation of the inductance at 100 kHz, which pumps the flux back and forth between readout and modulator loops, resulting in a 100-kHz

ac current through both loops. The ac current is coupled through a tuned circuit to a low-noise amplifier. A dc signal is generated by synchronous detection of the amplifier output. This dc signal serves as gyro readout signal and drives a feedback loop. The feedback loop generates a nulling field which is introduced through a dc transformer into the readout loop. The purpose of the nulling field is to drive the current in the loop to zero. This null method of readout provides high stability and linearity over a wide range for the readout and eliminates the torque on the gyro rotor from currents in the readout loop. The low-noise amplifier is a solid-state device located close to the gyroscope. The amplifier is enclosed in a miniature dewar (4 × 4 cm) to maintain proper operating temperature (200°K).

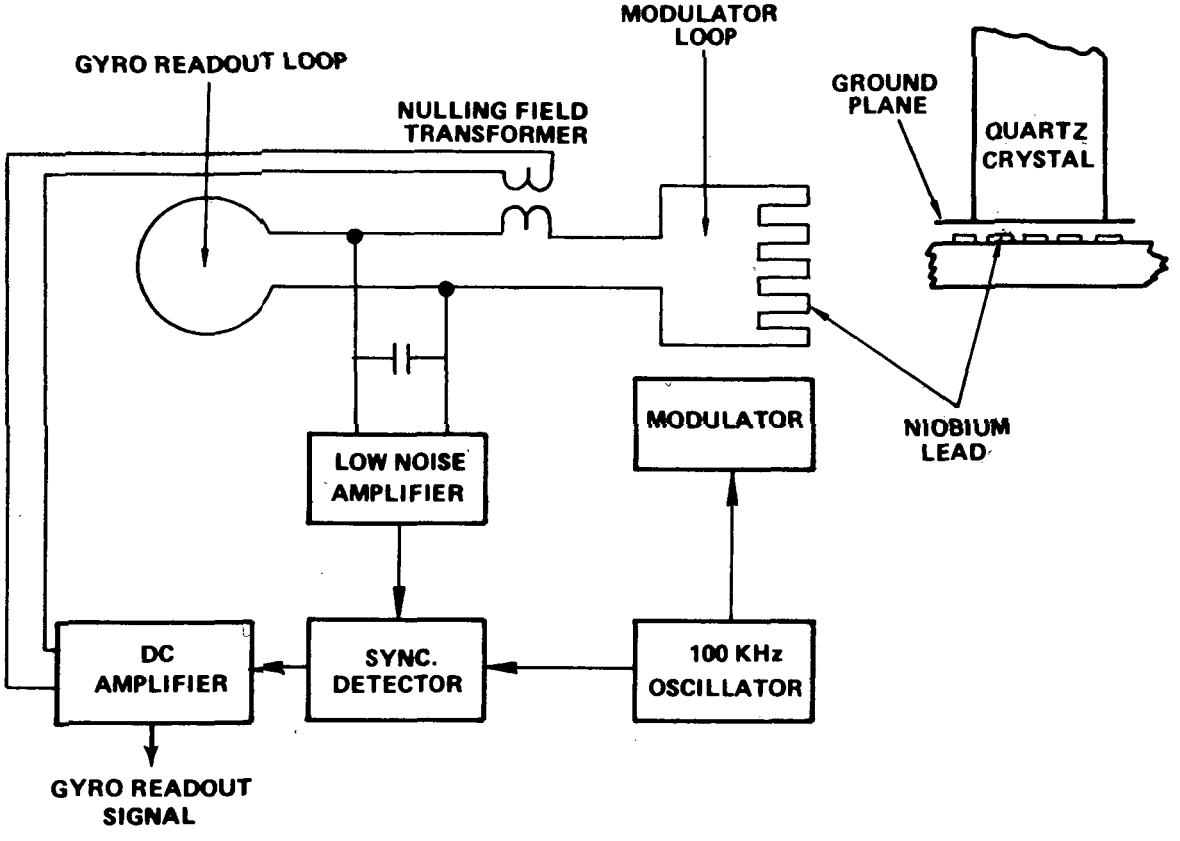

Figure 12. Gyro readout scheme.

In the Stanford/Honeywell gyro model, one readout loop is deposited on the separating surface of the gyro housing close to the rotor. A second

loop is contained on the retaining ring holding the gyro halves together. A third ring may be added to the outside of the housing. The three readout loops will be orthogonal to each other. Each loop consists of a thin layer of superconducting niobium.

To eliminate external magnetic fields, the gyro housing is enclosed in a superconducting shield provided by a spherical quartz shell covered with lead. Trapped magnetic flux inside the shield should be less than 10^{-6} weber (gauss cm^2) to reduce the magnetic torque on the gyro rotor to a sufficiently small amount. Trapped flux will be kept down by heat flushing during the cool-down process.

First readout tests on the gyro will be done using a Josephson junction magnetometer. The vibrating plane magnetometer described above is intended for the flight version of the gyro.

TELESCOPE AND STAR TRACKING

Telescope Design

The star-tracking telescope provides the reference direction in space against which the precession of the gyroscopes is measured. The telescope is locked on a star located near the celestial equator. The difference between the telescope readout and the gyro readout contains the relativistic gyro precession.

The telescope contains three spherical mirrors and a correction plate (Fig. 13). The optical path is folded three times by the mirror arrangement to obtain the short physical length of 0.33 m (13 in.). The short length of the telescope is important for mechanical stability. The effective focal length is 3.8 m (150 in.) with an aperture of 0.14 m (5.6 in.) and some central obstruction by the secondary mirror and beam splitter unit mounted on the correction plate.

Mechanical stability and rigidity of the telescope is of utmost importance to achieve desired null stability of 0.001 arc sec or better. All telescope parts are made of quartz, and the parts are connected together by optical contacting to eliminate the need of cementing. Even small changes in a cement film would affect the accurate alignment of

parts. The structural design of the telescope is shown in Figure 13. The primary and tertiary mirrors and the quartz tube are optically contacted to the mounting surface which serves as a reference plane. The gyroscopes are also mounted to this plate, and the plane of the gyro readout rings is aligned with respect to the mounting surface. A mechanical null stability of 0.001 arc sec corresponds to an image motion of about 2×10^{-5} mm for 3.8 m focal length. To achieve such a stability, temperature gradients across the telescope structure must be avoided. This is accomplished by the cryogenic environment provided by the liquid helium surrounding the telescope space. Material creep will be no problem in the zero-g environment of space. Relaxation of strain can be reduced properly by heat treatment of the telescope components. A preliminary analysis has shown that the required mechanical stability can be achieved in the space and cryogenic environment [5].

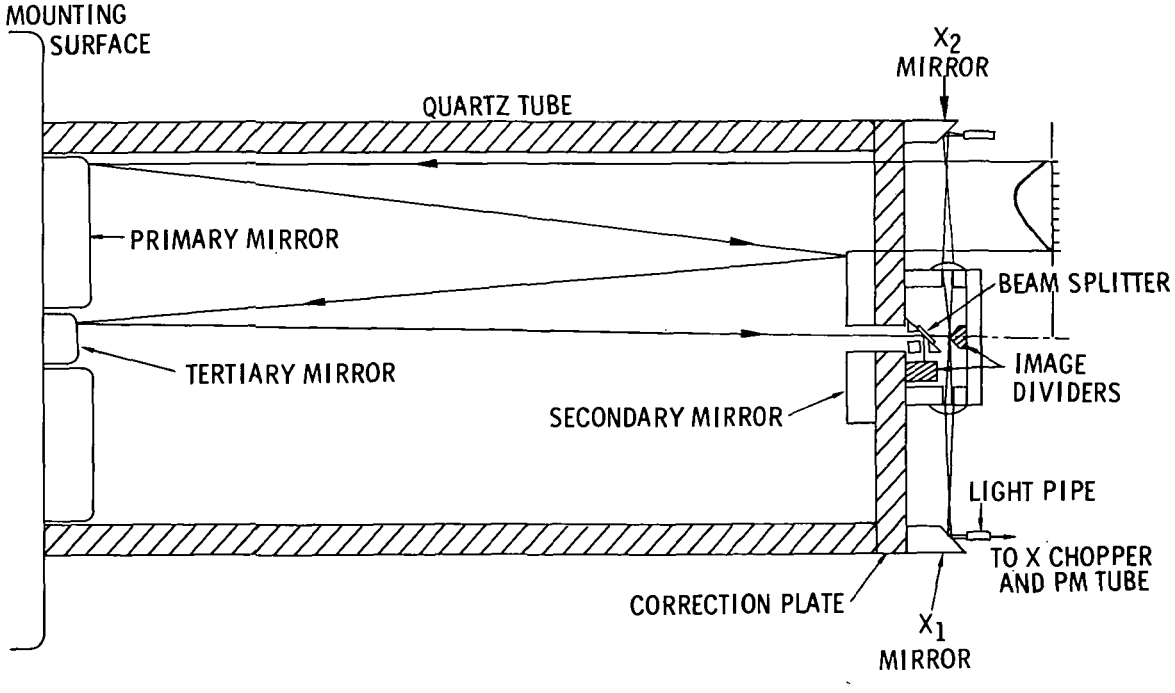

Figure 13. Telescope design.

Pointing Readout

The pointing angle of the telescope with respect to the reference star is obtained by a 2-axis readout system. The telescope readout signal is used as a reference for the gyro readout and in the attitude control system of the satellite. The light beam from the tertiary mirror passes through a hole in the center of the correction plate and through a beam splitter (Fig. 13). The two beams (X and Y) emerging from the beam splitter at right angles to each other are further divided at the edges of two roof prisms into a total of four light beams X_1, X_2, and Y_1, Y_2 (Fig. 14). Through this arrangement, the diffraction image of the reference star in the X and Y beams is divided into two halves by the edge of the roof prism. The intensity in corresponding beams (e.g., X_1 and X_2) is compared by a photomultiplier. If the telescope points exactly at the star, the image (beam) is centered on the edge of the image divider roof prism, and the resulting image halves (e.g., X_1 and X_2 beam) are of equal size and intensity. If a pointing error along the axis exists, the X_1 and X_2 beams have different intensities, and the X photomultiplier will generate an X-axis error signal. The same arrangement is true for the Y axis. The beam splitter arrangement is shown in Figure 14. Actually, the X_1X_2 beam and the Y_1Y_2 are located in different planes. The four light beams ($X_1X_2Y_1Y_2$) are reflected into four light pipes by small mirrors located at the circumference of the correction plate (compare Fig. 13). The lenses L provide for proper collection of the light beams by the light-pipe apertures.

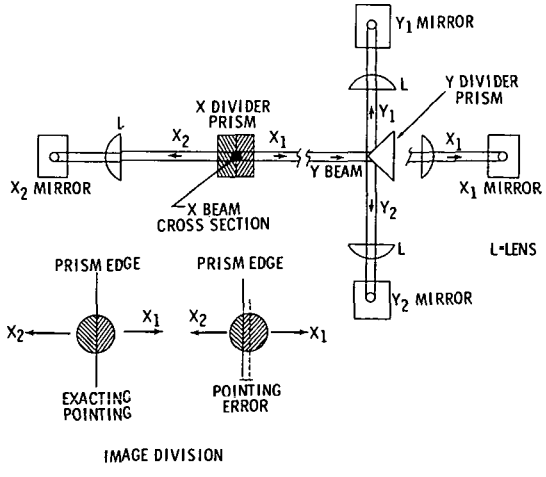

Figure 14. Beam splitter arrangement.

The four light pipes transmit the star light to two photomultiplier tubes (one for the X axis and one for the Y axis). The photomultiplier and associated electronics are located outside the cryogenic temperature area near the optical windows of the dewar. A rotating disk in front of each photomultiplier tube chops the light at a frequency of 50 Hz. Two semicircular slots in the chopper wheel permit the PM tube to look alternately at the output of two corresponding light pipes. The chopper wheel is driven by a

synchronous motor. The output signals from the photomultiplier tube are amplified and then passed through a blanking circuit which cuts off the signal for about 10 percent of time during the transition from X_1 to X_2 beams to eliminate spikes and erroneous signals (Fig. 15). If the telescope points exactly at the star, the X_1 and X_2 output signals of the PM tube are equal. If a pointing error exists along the X axis, the X_1 and X_2 signal levels are different (Fig. 15). The result is a 50-Hz ac signal which is amplified and detected synchronously to generate a dc error signal, with a magnitude proportional to the angular pointing error, and a polarity indicating the sign of the pointing error. The error signal passes through a gain-controlled amplifier which permits automatic adjustment of the scaling factor of the telescope readout. A timing signal for the blanking circuit and synchronous detector is generated by a lamp and photodiode in connection with two additional apertures in the chopper wheel. The described pointing readout system locates the center of the diffraction image of the star and generates the proper error signals which are then fed to the signal processing system. The reference star should be a bright star at or near the celestial equator with minimum proper motion. Rigel in Orion is one possible choice. For about half of the orbital revolution of the satellite, the reference star will be occulted by the earth. During this time, the attitude of the spacecraft will be controlled by the gyro signals to assure immediate acquisition of the star when it becomes visible.

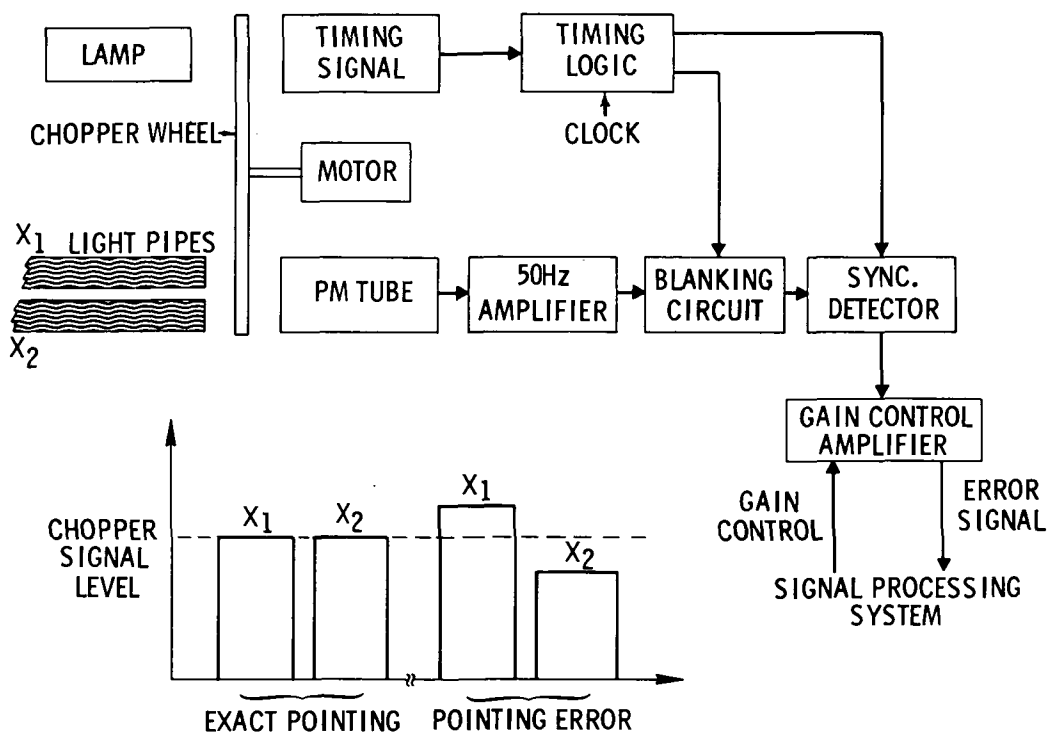

Figure 15. Telescope readout electronics.

Telescope Pointing

Telescope pointing and star tracking is accomplished by a dual-loop control system. The external servo-loop controls the attitude of the satellite to about one arc sec or less by means of the helium gas thrusters. The inner servo loop provides fine pointing of the telescope by cryogenic actuators. The telescope is mounted with flex pivots to the inside wall of the helium dewar which permits a few arc-sec motions of the telescope relative to the dewar vessel. The combined control loops will keep the telescope pointing within the linear range of the pointing readout (i.e., ± 0.05 arc sec from the center of the star image).

A separate star tracker/sun-sensor system will be used for initial orientation of the satellite and star acquisition.

DATA EXTRACTION

Experiment Data

The desired experiment data, i.e., the relativistic gyro precession, is contained in the difference between gyro and telescope readout. This difference signal contains several components, as indicated in Figure 16:

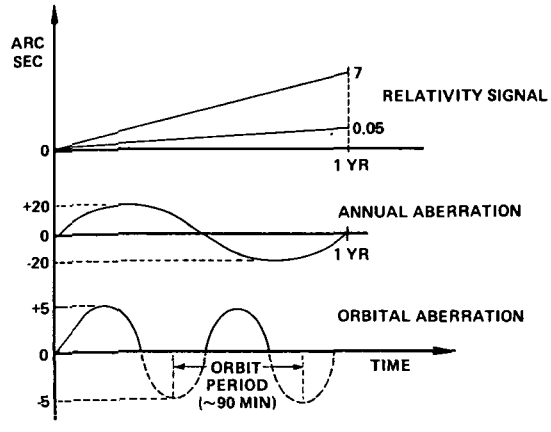

Figure 16. Gyro signal components.

a. The relativistic gyro precession is a continuously increasing signal reaching 7 arc sec and 0.05 arc sec after 1 year for the gyro orientations shown in Figure 1.

b. The annual aberration of star light is a sinusoidal signal with a period of 1 year and a maximum amplitude of ± 20 arc sec. It is caused by the motion of the earth around the sun.

c. The orbital aberration of starlight results from the motion of the satellite around the earth. It is a sinusoidal signal with a period of 90 minutes (orbital period) and a maximum amplitude of ± 5 arc sec. Only about half of this variation will be seen because of star occultation by the earth.

d. Noise from electronic circuits and attitude control.

The annual and orbital aberration can be calculated precisely and subtracted from the measurements. The orbital aberration signal provides a convenient periodic checkout and calibration of the gyro readout circuits.

A certain amount of signal and data processing must be done in the onboard equipment. Otherwise, prohibitive onboard data storage and data-transmission rates would be required. Assuming a readout range of ± 64 arc sec for the gyro with an accuracy of 0.001 arc sec requires a 17-bit digital word. With four gyros and readout of two axes each, eight data channels would be needed. If data sampling is done at 10-to 30-second intervals and data are transmitted to the ground once per day, the onboard memory has to store 10^4 to 10^5 words of 17 bits each of experiment data. The onboard storage requirements can be reduced by increasing the frequency of transmissions to the ground.

Signal and Data Processing

Figure 17 is a block diagram of the signal processing and data extraction system onboard the satellite. The system contains three loops: (1) data extraction loop, (2) calibration loop for telescope readout gain, and (3) attitude control loop. A reference generator provides synchronous signals for the operation of the system, and switching signals are generated by the control logic. The signals from the gyro and telescope readout circuits could be dc signals or ac signals (e.g., 50 Hz). It is assumed for the following discussions that both readout circuits provide dc signals.

Data Extraction Loop. The data processing path is indicated by the heavy lines in the block diagram of Figure 17. The telescope readout signal T and the gyro readout signal G are subtracted in the summing amplifier Z_1 which yields the output signal R = G - T; i.e., the desired experiment data. Attitude motions are cancelled out in the subtraction process, since gyro and telescope are mechanically an integral unit and experience equal attitude changes. To achieve true elimination of signals from attitude motions requires a response time of both readout circuits which is short compared to

attitude motions and the scaling factors of both readout circuits must be equal. Equalization of scaling factors is accomplished by the calibration loop discussed later.

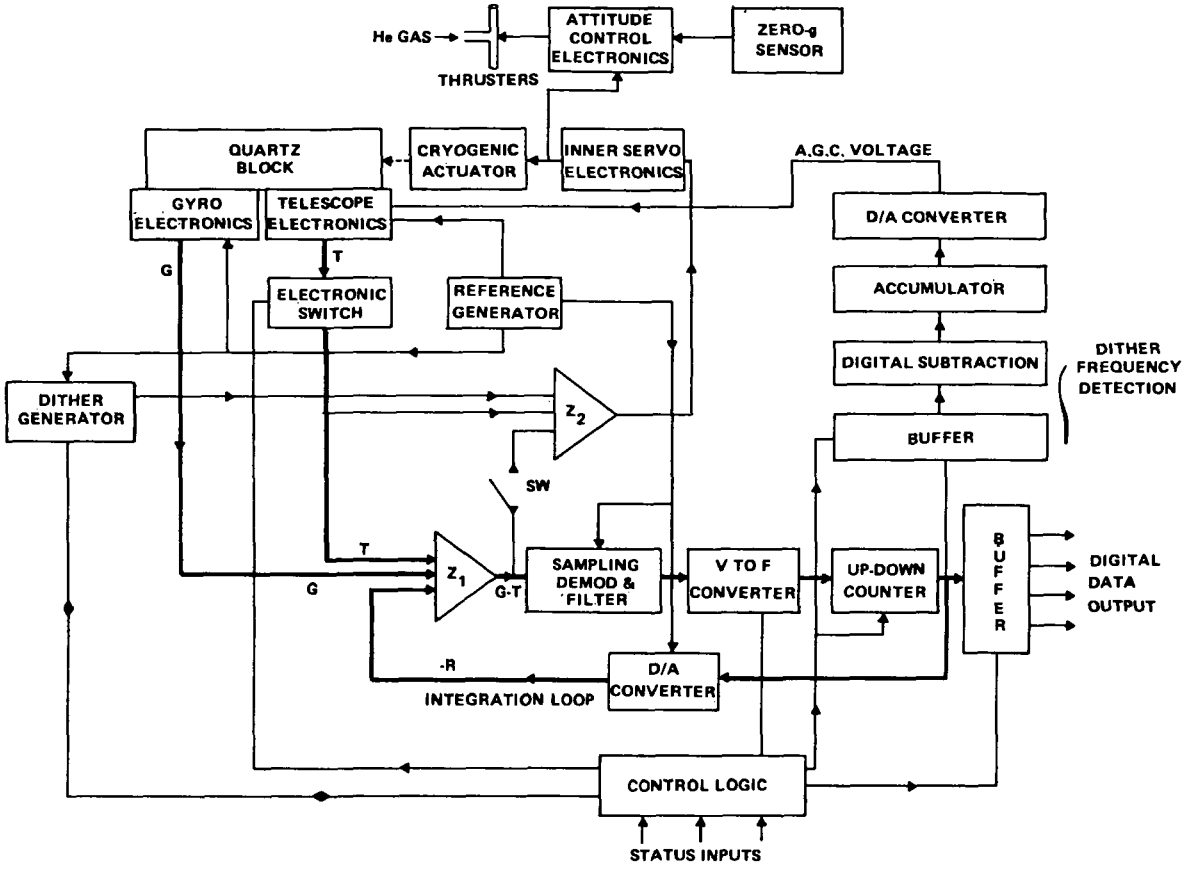

Figure 17. Signal and data processing.

The output of the Z_1 amplifier is converted into a digital signal by the voltage-to-frequency converter and the following reversible counter. The sampling, demodulator, and filter block should be omitted for analog signal processing assumed here. The reversible counter samples the G-T signal at 30-second intervals. The counter information is fed to a buffer storage from which it is transferred to the memory for storage and transmission to the ground.

The filtering of higher frequency noise in the difference signal is achieved by the integration loop containing the reversible counter and digital-to-analog converter. The output of the counter R = G - T is converted into an analog signal and fed back to the Z_1 amplifier to drive the output of Z_1 to zero (G - T - R). The signal R in the counter thus follows continuously

the G - T signal output of Z_1. The integrating loop has a time constant of about 10 seconds which suppresses high-frequency noise sufficiently but passes the orbital aberration signal (used for calibration). Recovery time of the system is about 1 minute.

During star occultation the electronic switch cuts off the telescope output signal. The reversible counter is inhibited; no data are accumulated and the buffer data are frozen. After star acquisition the reversible counter starts counting until the output of Z_1 is driven to zero by the feedback loop.

Calibration Loop. The data extraction scheme discussed before requires equal scaling factors in the gyro and telescope readout circuits. Changes in the gain of the telescope readout circuit can be expected since the sensitivity of photomultiplier tubes decreases due to aging. The calibration loop provides automatic adjustment of the telescope readout scaling factor to make it equal to the gyro scaling factor within the limit of one percent required to eliminate offset errors.

To compare the gain of both circuits, a dither signal is introduced into the inner servo loop which causes the telescope to sweep slowly forth and back across the star image over a range of about 0.03 arc sec at a rate of about 1/3 radians/sec. The small attitude motions caused by the dither signal will appear in the readout signal of the telescope and gyro. As long as both circuits have equal gain, the dither signal will be cancelled in the Z_1 summing amplifier (Fig. 17). When the gain of the telescope circuit changes, a dither signal will show up in the data loop. This dither frequency is detected synchronously at the output of the up-down counter and converted into an automatic gain control voltage (AGC) which adjusts the gain of the telescope circuit until the dither signal in the data loop disappears (i.e., equal gain in gyro and telescope circuit). The AGC is generated by digital sampling, subtraction, difference accumulation, and D/A conversion. The dither frequency is added to the telescope signal in the Z_2 amplifier.

The gyro readout circuit is inherently stable, and essentially no changes from aging should be expected. Absolute calibration of the gyro circuit is obtained from aberration signals. Offset in the data processing electronics should be less than 0.001 arc sec.

Attitude Control Loop. Fine pointing of the telescope/gyroscope assembly is accomplished by the inner servo loop and the cryogenic actuators (Fig. 17). The telescope readout signal is combined with the dither signal in the Z_2 summing amplifier, and the resulting signal is fed to the inner servo

electronics which controls the cryogenic actuators to track and center the star image in the telescope. Control signals from the inner servo electronics are tied into the attitude control system which switches the helium gas thruster for coarse attitude and zero-g control.

During occultation of the reference star the electronic switch cuts off the telescope output signal and fine pointing is controlled by the gyro signal through connection between Z_1 to Z_2 amplifier. Without the T-input signal the output of Z_1 is the gyro signal only. The switch SW will be open when attitude is controlled by telescope signals. The bandwidth of the inner servo loop permits the dither signal to pass through the loop.

The block diagram of Figure 17 represents the situation for a spacecraft without continuous roll. Only minor modifications will be required for a rolling spacecraft.

LIQUID HELIUM DEWAR

Flight Dewar

The liquid helium dewar provides the cryogenic environment for the experiment systems including the gyros, the telescope, and superconducting circuits. The low temperature is not only required to achieve superconductivity but also for temperature stabilization of the experiment. The cylindrical dewar will represent essentially the size and shape of the satellite. The liquid helium in the dewar will provide a constant low temperature environment (1.6°K) in space for at least 1 year. The gas boiling off from the liquid helium will be used in the attitude control system of the satellite. The dewar must be made of nonmagnetic materials.

The flight dewar has not been designed yet, but a smaller size laboratory model with all important features of the flight dewar has been built for development of the experiment. The following physical parameters are estimates for the flight liquid-helium dewar:

Mass (dry): 200 kg (450 lb)

Size: Diameter - 1.26 m (50 in.)
Length - 1.65 m (65 in.)

Helium content: 140 kg (300 lb) or 1120 liter

Total mass: 340 kg (750 lb)

The simplified sketch in Figure 18 illustrates the basic features of the dewar. The inner vessel contains the experiment systems and the liquid helium. To minimize heat transfer from the outside into the system, the inner vessel is supported in the outer vessel by thin wires or tapes. The experiment space, containing the telescope and gyros, is evacuated (open to space). The experiment space is surrounded by superfluid helium (1.6°K). The light from the star enters the dewar and telescope through two quartz windows coated with a film of gold to reflect thermal radiation but transmit visible light. The sun shield prevents direct thermal radiation input from the sun and other sources.

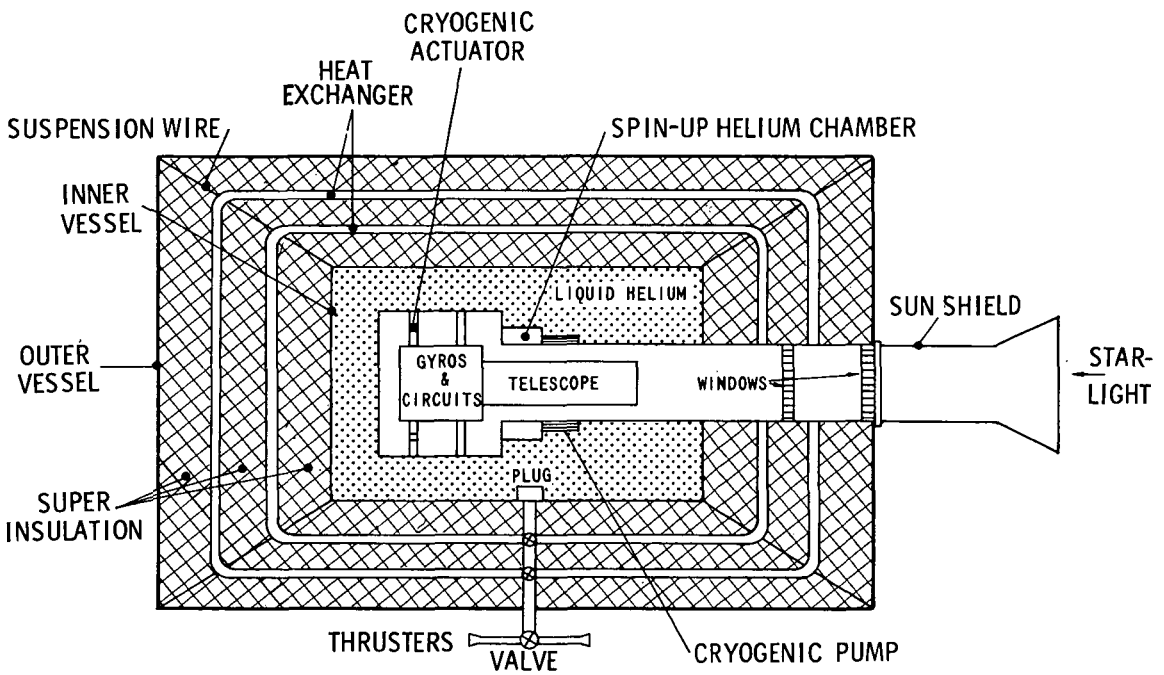

Figure 18. Helium dewar concept.

The space between the inner and outer vessel contains two heat exchangers embedded in layers of superinsulation. During launch, the inner vessel is supported by retractable rods since the superinsulation is compressible and cannot provide the necessary support for the inner vessel.

Once in orbit, the retractable rods are removed. The heat input into the inner vessel from heat leaks in the superinsulation, from radiation through the telescope windows (which is the largest contribution), and other sources will cause the helium to boil off at a low rate. The venting and refrigeration of the liquid helium container is accomplished in a unique way by exploiting the properties of superfluid helium [6]. The inside wall of the helium container is covered by a film of superfluid helium. The outlet of the container is provided by a plug which contains very fine pores and has extremely high thermal conductivity. Helium flows through the plug at a rate determined by the pressure and temperature differences. When it reaches the outer surface of the plug, it evaporates and cools the plug refrigerating the vessel through the high thermal conductivity of the plug. In this way, refrigeration of the helium container is obtained, and the problem of separating liquid and gas for venting under zero gravity conditions is circumvented. With suitable design, the plug will successfully control the flow of either normal or superfluid helium. Uniform temperature equilibrium within the dewar is maintained through the high thermal conductivity of the superfluid helium film.

The helium gas evaporating from the superfluid plug passes through two heat exchangers consisting of copper shields with coiled tubing surrounding the inner vessel. The refrigeration obtained from the two heat exchangers increases the hold time for liquid helium by a factor of 20 to 25 compared to a dewar without heat exchangers. A third heat exchanger would yield an additional gain of 15 to 20 percent, but would increase the complexity of the system. The inner heat exchanger operates at a temperature of about 35°K. The outer heat exchanger operates at 125°K (assuming room temperature outside the dewar). From the heat exchanger, the helium gas is fed to a number of valves which control the gas flow through twelve jet nozzels for attitude control and nonpropulsive venting.

The gyro spin-up is accomplished with helium gas which is boiled off from an annular chamber surrounding the telescope. The helium gas is fed through pipes from the chamber to the spin-up channels in the gyro housing. The exhaust gas from the spin-up channels is vented into space. Spin-up of the gyros will be done in orbit. During flight, the vacuum in the inner vessels is maintained below 10^{-9} mm Hg by connecting the volume of the inner vessel with the vacuum of space and by additional cryogenic pumping. The cryogenic pumping is accomplished by using material (e.g., charcoal) which absorbs molecules at low temperature. The final design of the flight dewar will probably consist of a dual dewar system with a separable inner dewar of about 0.4-m (16-in.) diameter containing the

experiment hardware. The smaller volume of the inner dewar simplifies the problem of obtaining low trapped magnetic fields in the superconducting shields of the gyroscopes. In addition, the dual dewar concept reduces the stringent requirements on magnetic properties for the main satellite dewar and allows parallel development and testing of the main satellite dewar and experiment package.

Laboratory Dewar

A laboratory-model dewar has been built to test the concept of the flight dewar and to provide the cryogenic environment for ground testing and simulation of the experiment. The laboratory dewar incorporates the essential features required for the flight dewar but deviates in mechanical design from what would be considered optimum for the flight dewar. Governing design requirements for the laboratory dewar were easy access to the inner components of the dewar, ease in assembly and disassembly as required for laboratory testing, mechanical stability for the 1-g environment to keep alignment between inner and outer parts within 1 arc sec, and operation capability in any position (horizontal or vertical) including rotation about the axis.

The size of the laboratory dewar is 0.76 m (30 in.) in diameter and 1.45 m (57 in.) long with a mass of 350 Kg (800 lb) and a liquid helium capacity of about 140 liters. The dewar will hold liquid helium for about 100 days on earth. The more rigid mechanical design results in a larger heat input into the dewar, compared to the flight configuration. To obtain mechanical stability, the inner vessel of the dewar is supported by a stiff, 22 cm (9-in.) diameter neck tube and by a mounting ring attached at the center of gravity of the inner vessel. The mounting ring is connected to the outer vessel of the dewar through twelve alignment bolts with 2.5-mm (0.1-in.) diameter which provide a means to align the inner vessel during low-temperature operations. An outside mounting ring is provided to support the dewar at the center of gravity in a telescope mount for experiment simulation and testing.

For initial evacuation of the inner vessel (during gyro spin-up), the quartz window covering the neck tube is raised 3 inches and a 10-inch diffusion pump is connected to the neck tube. The 0.38-m (1.5-in.) diameter exhaust pipe from the spin-up channel is connected to a high-speed mechanical pump. After completion of the gyro spin-up, the window and valves are closed, the pumps are removed, and the vacuum is maintained below 10^{-8} mm Hg using an

ion pump mounted near the window.

The helium gas boiling off from the superfluid plug is fed to two heat exchanger systems inside the superinsulation operating in parallel. The gas flow distribution through the two heat exchanger systems can be adjusted according to the heat load. The helium gas is then taken off through a rotary seal at the bottom of the dewar.

REFERENCES

1. Schiff, L. I.: Motion of a Gyroscope According to Einstein's Theory of Gravitation. Proc. Nat. Academy of Sciences, vol. 46, 1960, pp. 871-882.

2. Everitt, C. W. F.: The Stanford Gyroscope Experiment. Proceedings of the conference on Experimental Test of Gravitation Theories, Jet Propulsion Laboratory, California Institute of Technology, November 1, 1971.

3. Bracken, T. D. and Everitt, C. W. F.: Design of Gas Spin-Up System for an Electrostatically Supported Cryogenic Gyroscope. Adv. Cry. Eng., 13, 168, 1968.

4. Opfer, J. E.: Modulated Inductance Magnetometer. Rev. de Phys. Applique, 5, 37, 1970.

5. Everitt, C. W. F. and van Patten, R. A.: Status of Development of the Startracking Telescope for the Relativity Experiment. Internal Publication, Stanford University, 1968.

6. Selzer, P., Fairbank, W. M., and Everitt, C. W. F.: Adv. Cry. Eng., 16, 1971.

APPROVAL

GYROSCOPE RELATIVITY EXPERIMENT

By Rudolf Decher

The information in this report has been reviewed for security classification. Review of any information concerning Department of Defense or Atomic Energy Commission programs has been made by the MSFC Security Classification Officer. This report, in its entirety, has been determined to be unclassified.

This document has also been reviewed and approved for technical accuracy.

Gerhard B. Heller

GERHARD B. HELLER
Director, Space Sciences Laboratory

DISTRIBUTION

INTERNAL

DIR
Dr. Rees

DEP-T
Dr. Lucas

AD-S
Dr. Stuhlinger

A&TS-PAT
Mr. L. D. Wofford, Jr.

A&TS-MS-H

A&TS-M-IP (2)

A&TS-M-IL (2)

A&TS-TU (2)

PD-DIR
Mr. Downey

PD-MP-S
Mr. William T. Roberts

PM-PR-M

S&E-DIR
Dr. Weidner

S&E-DIR
Mr. Richard

S&E-PT-DIR
Dr. Siebel

S&E-PT-M
Mr. Angele

INTERNAL (Continued)

S&E-CSE-DIR
Dr. Haeussermann

S&E-ASTR-DIR
Mr. Moore

S&E-ASTR-G
Mr. Mandel
Dr. Doane

S&E-AERO-DIR
Dr. Geissler

S&E-ASTN-DIR
Mr. Heimburg

S&E-ASTN-P
Mr. Paul

S&E-SSL-DIR
Mr. Heller

S&E-SSL-X
Mr. Winkler

S&E-SSL-C

Reserve (15)

S&E-SSL-T
Mr. Snoddy

S&E-SSL-P
Dr. Naumann

S&E-SSL-P
Mr. Holland

DISTRIBUTION (Concluded)

INTERNAL (Concluded)

S&E-SSL-S
Dr. Sieber

S&E-SSL-S
Mr. Jones

S&E-SSL-S
Mr. Katz

S&E-SSL-N
Dr. Decher (20)

S&E-SSL-N
Mr. Stern

S&E-SSL-N
Dr. Edmonson

S&E-SSL-N
Dr. Eby

S&E-SSL-N
Mr. Wills

S&E-SSL-N
Dr. Urban

S&E-SSL-N
Dr. Parnell

S&E-SSL-N
Mr. Burrell

S&E-SSL-N
Mr. Peasley

S&E-SSL-N
Dr. Peters

EXTERNAL

Washington, D. C.
NASA Headquarters
Code SG/Mr. Jesse Mitchell
Code SG/Mr. Dixon Ashworth
Code SG/Dr. Nancy Roman

W. W. Hansen Labs of Physics
Department of Physics
Stanford University
Stanford, California 94305
Dr. F. Everitt
Dr. W. Fairbank

Durand Laboratory
Department of Aeronautics &
Astronautics
Stanford University
Stanford, California 94305
Dr. D. DeBrae
Mr. D. van Patten
Dr. W. Pondrom

Scientific and Technical Information
Facility (25)
P.O. Box 33
College Park, Maryland 20740
Attn: NASA Representative (S-AK/RKT)

MSFC—RSA, Ala